Jurnal Tribologi 20 (2019) 97-113

MYTRIBOS Malaysian Tribology Society

Jurnal Tribologi

Website : jurnaltribologi.mytribos.org e-issn: 2289-7232

Macroscopic tribological properties of thick concentrated polymer brush on rough steel under lubrication with ionic liquid

Keisuke Sato [1,*], Hikaru Okubo [1], Yuki Hirata [2], Chiharu Tadokoro [3], Ken Nakano [4], Yoshinobu Tsujii [5], Shinya Sasaki [6]

[1] Department of Mechanical Engineering, Graduate school of Tokyo University of Science, 1258585 Tokyo, JAPAN.
[2] Department of Mechanical Engineering, Tokyo Institute of Technology, 1528550 Tokyo, JAPAN.
[3] Department of Mechanical Engineering, Saitama University, 3388570 Saitama, JAPAN.
[4] Department of Mechanical Engineering, Yokohama National University, 2408501 Kanagawa, JAPAN.
[5] Kyoto University Institute for Chemical Research, 6110011 Kyoto, JAPAN.
[6] Department of Mechanical Engineering, Tokyo University of Science, 1258585 Tokyo, JAPAN.
*Corresponding author: 4517620@ed.tus.ac.jp

KEYWORD

Concentrated Polymer Brush
Ionic Liquid
Polymer
Low friction
Rough steel

ABSTRACT

Concentrated polymer brush (CPB) is the polymer film with a structure that possesses greatly extended polymer chains densely grafted to substrate. CPB is known to swell in good solvents, which have high affinity for the polymer. Swollen CPB by a good solvent shows excellent micro-tribological properties such as super lubrication with the extremely low friction coefficient ($\mu \sim 10^{-4}$). However, macro-tribological properties of CPB surface on steel have not been explored sufficiently. In this study, macroscopic tribological properties of a CPB on rough steel were evaluated using a block-on-ring type tribo-tester under lubrication with an ionic liquid. The CPB showed a significant friction reduction effect with the low friction coefficient of 0.005 on macroscale.

1.0 INTRODUCTION

The use of organic molecules, such as oiliness agent, has been one of the well-known approach to improve friction and wear characteristics of sliding components. Boundary lubrication layer models derived from oiliness agent have been proposed by Hardy and Allen and a mono- or multi-molecular layer of oiliness agent on sliding surfaces can prevent solid-solid contacts between two

Received 29 June 2018; received in revised form 10 September 2018; accepted 25 September 2018.
To cite this article: Sato et al. (2019). Macroscopic tribological properties of thick concentrated polymer brush on rough steel under lubrication with ionic liquid. Jurnal Tribologi 20, pp.97-113.

contacting surfaces, resulting in low friction at sliding interfaces (Allen and Draugils, 1969; Hutching, 1992).

In accordance with the low frictional concept, the formation of organic compounds over the sliding surfaces is one of the greatly effective approach. They are firmly anchored to sliding surfaces and have a low shear strength. Thus, it can contribute to achieve low friction. In such a back ground, polymer-coated surfaces, such as polymer brushes, have been attracted much attention owing to their unique characteristics (Parnas and Cohen, 1994; Klein and Kumacheva, 1995; Klein, 1996; Yang and Zhou, 2017; Chen, W et al., 2017; Murdoch et al., 2018). Lubrication with polymer brushes has been reported by several researchers (Klein, 1994; Klein et al., 1994; Irfachsyad et al., 2002; Bielecki et al., 2012). It has been proposed that the friction reduction mechanism for polymer brushes can be mainly attributed as the following three: (a) repulsive terms consisting osmotic pressure within polymer brushes (b) confinement of lubricant in polymer brushes (c) the formation of a low-shear layer in the outer reaches of polymer brushes (Irfachsyad, 2002; Bielecki et al., 2012). Over the last decade, high-density and well-defined polymer brushes, or concentrated polymer brush (CPB) have been synthesized via surface-initiated atom transfer radical polymerization (SI-ATRP). One of the advantages of SI-ATRP, also known as the "grafting from" method, is superior adherence to substrates, which means that polymer chains are strongly anchored to substrates. Thus, this "grafting from" structure is potentially stable to solvent or tribological stress. Tsujii et al (2009) reported that CPB of PMMA in a good solvent exhibited extremely low friction coefficient ($\mu \sim 10^{-4}$) under a load of 25 nN using atomic force microscope (AFM). Sakata et al (2005) reported that the PMMA brush prepared by SI-ATRP exhibited better wear resistance compared to those prepared by spin-coating, and a low friction coefficient of 0.05 against a stainless ball under a contact pressure of 200 MPa. Due to these excellent tribological properties, CPB has been expected to be applied to macroscopic mechanical components in industrial fields.

On the other hand, there are several issues to apply CPB to practical mechanical components. One of these issues is that most of mechanical components are normally constituted of ferrous-based materials with relatively high roughness. However, many reports on CPB, such as mentioned above, focused on the tribological properties of CPB coated on a smooth surface (mainly Si wafer or glass). Few reports (Bielecki et al., 2013; Kobayashi, 2016) are available on the tribological properties of polymer brushes on ferrous-based materials. Moreover, it should be noted that few studies have focused on the effects of surface roughness on tribological properties of CPB. It is not clear whether excellent tribological characteristics of CPB exhibit or not for applying CPB to practical mechanical components. Therefore, it is important to investigate the macroscopic tribological properties and the durability of CPB coated on ferrous-based substrate with relatively high roughness, and organized tribological studies are absolutely needed to apply CPB to ferrous-based sliding components. There is another problem, which is that most of good solvents conventionally used for polymer brushes, such as organic solvents or water, have high volatility and low viscous. It is easily expected that polymer brushes with these solvents have difficulty maintaining a low friction for a long sliding distance. Therefore, it is necessary to explore the combination of CPB and new solvents for demonstrating CPB's full ability.

Ionic liquids have attracted much attention as innovative solvents. Ionic liquids are molten salts composed of cations and anions. Several studies have reported that they have excellent characteristics such as high thermal stability, high viscosity, non-volatility, non-combustibility and electrochemical stability (Dupont, 2002; Freemantle, 2009; Kirchner, 2010). Ionic liquids can dissolve various kinds of materials, including some polymer materials, owing to the chemical

structures of the constituent anionic and cationic species (Carmichael, 2000; Biedron, 2001; Susan, 2005; Kubisa, 2009). The use of ionic liquids in tribology has also been expected. Their tribological properties as based-fluid have been evaluated (Liu et al., 2002; Minami, 2009) and some of the ionic liquids exhibited good friction reduction and anti-wear properties. Due to their unique properties as mentioned above, the use of ionic liquids as good solvents for polymer brushes has attracted attention. Nomura et al (2012) demonstrated that PMMA brushes exhibited a low friction coefficient in ionic liquids as a result of AFM measurement. Arafune et al (2015) reported that high density ionic liquid polymer brushes showed low friction coefficient ($\mu_{min} \sim 10^{-3}$) under a normal load of 14.7 N in an ionic liquid. Hence, ionic liquids can be appropriate for good solvents for polymer brushes.

In the context, it is expected that the combination of CPB and ionic liquid will be newly super-low frictional tribo-system. However, the macro-tribological performance of CPB on ferrous-based materials lubricated with ionic liquids has little been investigated. The clarification of the macroscopic tribological performance of CPB will give us beneficial information to design newly low frictional CPB's tribo-system and achieve the application of CPB to sliding components in industrial fields. In this work, a thick concentrated PMMA brush was synthesized on steel having high roughness, and the macro-tribological properties of the CPB under lubrication with an ionic liquid were evaluated.

2.0 EXPERIMENTAL SECTION

2.1 Materials

An AISI 52100 ring and an AISI 52100 block were used as test pieces. The radius and width of the ring test piece were 30.0 mm and 3.8 mm, respectively. The width, depth, and height of the block piece were 6.4 mm, 16.6 mm, and 9.7 mm, respectively. The surface roughness R_a of the block piece and the ring piece were 0.526 ± 0.028 μm and 0.521 ± 0.047 μm, respectively.

The compounds as follows were used for synthesis of concentrated PMMA brush via SI-ATRP. MMA (Nacalai Tesque Inc., JP) was purified by distillation. Ethyl 2- bromoisobutyrate (EBIB) (Tokyo Chemical Industry Co., Ltd., JP) was used as received. (2-bromo-2-methyl)propionyloxypropyltriethoxysilane (BPE) was used as an initiator for graft polymerization. 4.4'-Dinonyl-2,2'-bipyridine (Dn-bipy) (Aldrich, US) was purified by recrystallization in ethanol. Copper bromide (CuBr) and Copper dibromide ($CuBr_2$) (Wako Pure Chemicals, JP) were used as received.

An ionic liquid used as a lubricant was *N*,*N*-diethyl-*N*-methyl-*N*-(2-methoxyethyl)ammonium bis (trifluoromethanesulfonyl)imide (DEME-TFSI) supplied by Kanto Reagents (Tokyo, Japan), which has been found to be a good solvent for concentrated PMMA brush (Nomura, 2012). The viscosity of DEME-TFSI is 67 mPa・s at 298 K.

2.2 Synthesis of concentrated PMMA brush via SI-ATRP

A concentrated PMMA brush was synthesized via SI-ATRP method. Prior to the SI-ATRP process being undertaken, all the test pieces were washed with a mixed solution of acetone and hexane, chloroform, and 2-propanol in that order for 30 minutes each. A BPE solution was prepared at a ratio of BPE : EtOH : NH_3(aq) = 1:89:10 (wt%). All the test pieces were immersed in the BPE solution for 6 hours to immobilize BPE on the surface of the test pieces. After 6 hours passed, all the test pieces were washed with ethanol for 30 minutes. The reaction mixture for the

polymerization was prepared at a ratio of EBIB : MMA : CuBr : CuBr2 : Dn-bipy = 9.6×10^{-4}:98:0.23:0.039:1.4 (wt%) in a glove box with argon. Polymerization reactions were carried out at 333 K and 400 MPa for 4 hours. After the polymerization, all the test pieces were washed with tetrahydrofuran (THF) for 30 minutes to remove the free polymer adsorbed to the test pieces.

2.3 Characterization of concentrated PMMA brush

Number-average molecular weights M_n of the free polymers which were simultaneously produced from the initiator added to the reaction mixture was 3,758,046 as determined by gel permeation chromatography (GPC) (Shodex GPC-101, JP). There have been reports that the molecular characteristics of the free polymers closely approximate those of the graft polymers (Werne, 1999; Werne, 2001; Blomberg, 2002; Pyun, 2003). Therefore, it is considered that M_n of the polymer grafted to each test pieces is equivalent to M_n of the measured free polymer. The film thickness L_d of the CPB grafted to both test pieces could not be measured by an ellipsometer (M-2000U, J.A.Woolam, Lincoln, NE), due to the rough surface of both test pieces. Graft density σ of CPB is evaluated according to the equation (1) below:

$$\sigma = \frac{dL_d N_A}{M_N} \tag{1}$$

where d, L_d, N_A and M_N are assumed density of bulk PMMA at 293 K (1.19 g cm^{-3}), film thickness of the CPB, Avogadro's number, and number-average molecular weights of the free polymers, respectively. As mentioned above, it is difficult to measure the film thickness L_d of the CPB grafted to the both test pieces by using the ellipsometer due to high roughness. Therefore, the film thickness L_d of the concentrated PMMA brush grafted to a mirror polished AISI 52100 disk (the diameter and thickness of the disk were 24 mm and 7.9 mm, respectively. R_a = 0.017 ± 0.001 μm) under the same polymerization condition was used as a reference value, which was 700 ± 9.7 nm averaged by the value obtained at three different positions of the CPB grafted to the mirror polished steel disk in dry conditions (non-swelled), and M_N was 2,909,120 as a result of GPC measurement. From these values and the above equation, calculated graft density is 0.172 ± 0.024 chains/nm^2. The mechanical properties of the CPB were also measured by a triboindenter (Bruker Ti-950, US), with a Berkovich diamond indenter. According to this measurement, the indent depth was set to 50 nm considered to be 1/10 or less of the film thickness to avoid the influence of the substrate, and mechanical properties were estimated by the method proposed by Oliver and Pharr (1992). The measured characteristics of the CPB are listed in Table 1.

Table 1: The measured characteristics of the CPB

Parameter		Values
Film thickness	[nm]	700±9.7[a)]
Graft density	[chains/nm^2]	0.172±0.024[a)]
Hardness	[GPa]	0.431±0.034
Elastic modulus	[GPa]	9.30±0.53

[a)] The reference value of CPB grafted to AISI 52100 disk.

2.4 Block-on-ring tribological test

Macroscopic block-on-ring type friction tests were conducted under lubrication with the ionic liquid by means of a tribometer (Bruker UMT, US) as shown in Figure 1. The applied load was maintained at 2 N. 10 sliding speed values were selected between 0.0008 ms^{-1} and 1.6 m s^{-1} to acquire the Stribeck curve for the CPB. At each speed, friction coefficient values were averaged for 2 minutes. Measurements were conducted at 298 K. The sliding materials combinations were constituted four combinations of block/ring: Steel/Steel, CPB/steel, steel/CPB and CPB/CPB, as shown in Figure 2. In order to confirm repeatability of the frictional behavior, 5 cycles of tests were conducted for the tribopairs including CPB (CPB/Steel, Steel/CPB, CPB/CPB), and three tests for the Steel/Steel tribopairs.

Moreover, another friction test was conducted to investigate the durability of the CPB using the block-on-ring type tester. The test was conducted under a load of 2 N at a sliding speed of 0.8 ms^{-1} under lubrication with the ionic liquid. Measurements were conducted at 298 K. The sliding materials combinations were two combinations of Steel/Steel and CPB/CPB. In this test, the CPB was immersed in the ionic liquid for 5 h, in advance.

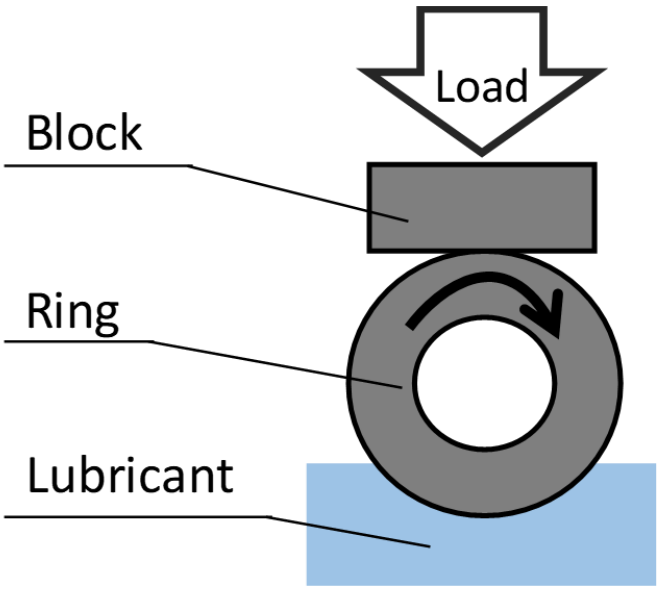

Figure 1: Schematic illustration of block-on-ring type friction test under lubrication with ionic liquid.

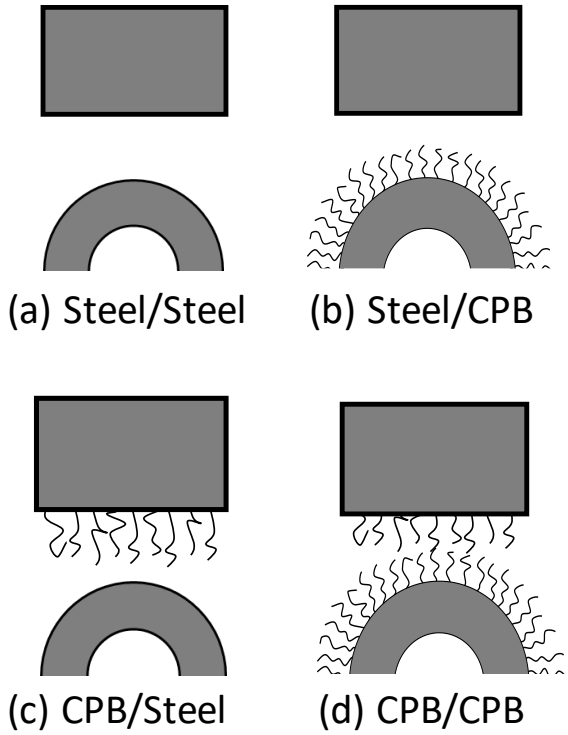

Figure 2: Schematic illustration of the four combinations of block/ring: (a) Steel/Steel (b) Steel/CPB (c) CPB/Steel (d) CPB/CPB.

2.5 Surface analysis

After the Stribeck-curve friction test, the wear scar of the block test pieces was evaluated by confocal laser scanning microscopy (VK-X 150, KEYENCE, Japan).

After the durability friction test, the backscattered electron image of the CPB grafted to the block test piece was obtained with scanning electron microscopy energy dispersive X-ray spectroscopy (SEM-EDS) (HITACHI TM3030Plus, JP) using 15.0 kV accelerating voltage. All analyses were conducted on the block test piece since the ring test piece could not be inserted into an analysis chamber.

2.6 Wettability evaluation

The wettability of the ionic liquid to the disk and the CPB was evaluated to clarify the retention effect of the lubricant of each material. A contact angle analyzer (Surface & Electro Optics Co.,Ltd Phoenix 300 Touch, KOR) was used. Droplet of the same amount of the ionic liquid were dropped onto each test piece, and an optical microscopic image of the droplet on the surface of each test piece was obtained. The contact angle of the ionic liquid to each test piece was obtained from the optical microscopic image by a half-angle method (Williams et al., 2010).

3.0 RESULTS

3.1 Stribeck curves for all tribopairs lubricated with the ionic liquid

In order to understand the role of tribopairs, Steel/Steel, CPB/Steel, Steel/CPB and CPB/CPB tribopairs were tested in the ionic liquid. Friction versus sliding speed (Stribeck) curves were obtained for all tribopairs.

The Stribeck curves for each tribo-combination per cycle are shown in Figure 3-6 [Steel/Steel, CPB/Steel, Steel/CPB and CPB/CPB (block/ring), respectively]. From Figure 3-6, the different friction behaviour was observed depending on the tribopairs.

For the Steel/Steel and CPB/Steel tribopairs, a high friction coefficient of approximately 0.2 at low sliding speed was observed regardless of sliding cycles, indicating that the friction test at low sliding speeds was completely operated under boundary lubrication regardless of whether the CPB was coated on the block test piece or not. Moreover, the friction coefficient of the Steel/Steel and CPB/Steel tribopairs decreased with the increment of the sliding speed for all the test cycles. This tendency was characterized as the transition of the boundary lubrication to mixed lubrication, which suggests that a low frictional EHL separating film is only formed at high sliding speeds. It should be noted that the frictional behaviour for this two tribopairs hardly changed depending on the cycles. From the results, the CPB coated on the block test piece hardly contributed to the friction reduction under the friction test condition.

On the other hand, the great contribution of the CPB to low friction was observed for the Steel/CPB and CPB/CPB tribopairs. In Figure 5 and 6, for the first frictional cycle, the Steel/CPB and CPB/CPB tribopairs gave a high friction coefficient of approximately 0.18 at the low speed region. In similar way to the case of the Steel/Steel and CPB/Steel tribopairs, the friction coefficient gradually decreased with the increment of the sliding speed and reached the value of 0.03-0.07 in the high-speed region. After the first cycle, it is interesting to note that the high friction coefficient in the low-speed region gradually decreased as the number of test cycles increased, and a low friction coefficient of 0.02 was confirmed on the 5^{th} cycle, regardless of the sliding speed for the Steel/CPB and CPB/CPB tribopairs. This clearly indicates that the existence of the CPB on the ring test piece contributed to form a low frictional lubrication layer regardless of the sliding speed.

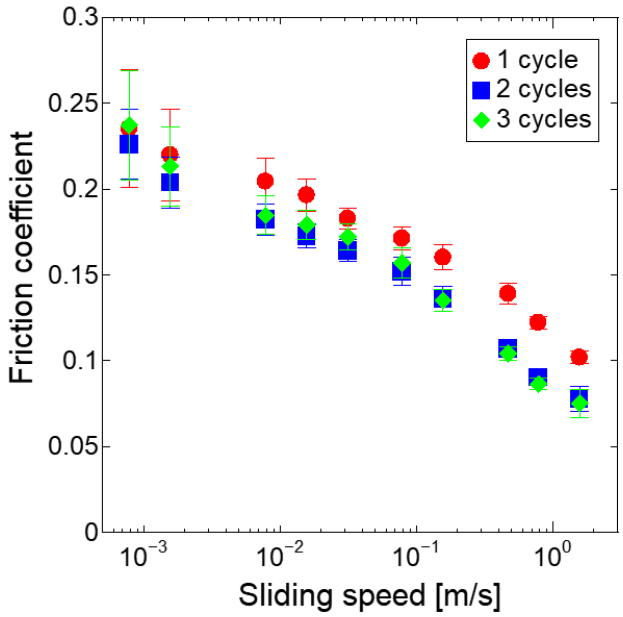

Figure 3: Friction coefficient of Steel/Steel tribopair as a function of sliding speed per each cycle.

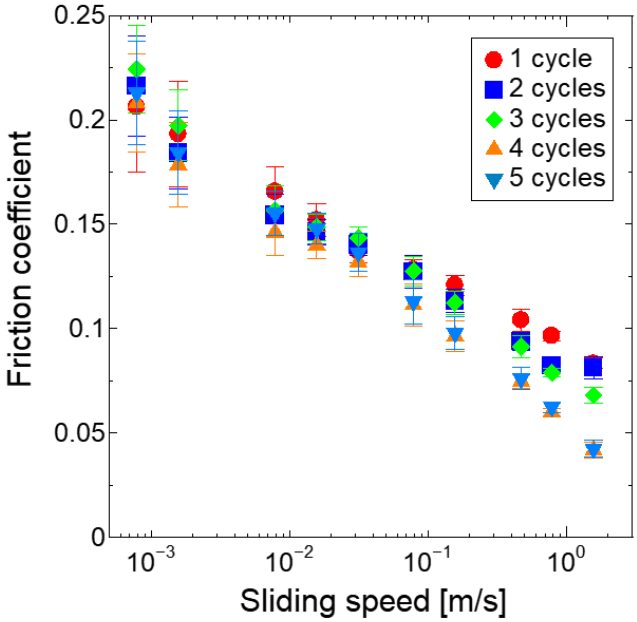

Figure 4: Friction coefficient of CPB/Steel tribopair as a function of sliding speed per each cycle.

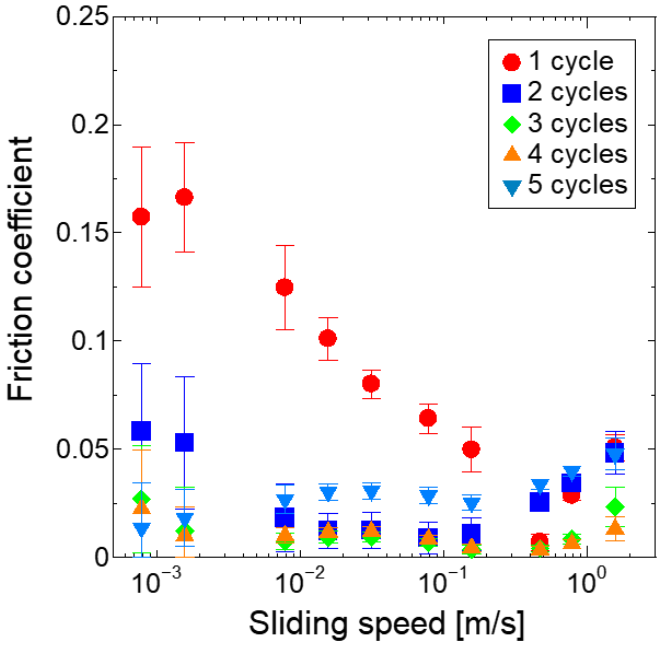

Figure 5: Friction coefficient of Steel/CPB tribopair as a function of sliding speed per each cycle.

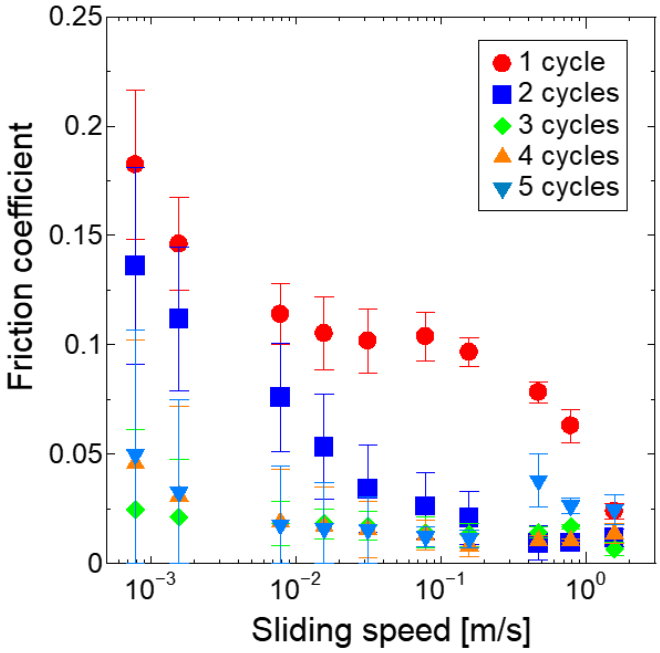

Figure 6: Friction coefficient of CPB/CPB tribopair as a function of sliding speed per each cycle.

Figure 7 shows the optical observation images and the change of the surface roughness R_a ratio that was defined as the ratio of the surface roughness of the block test pieces for the steel and the CPB block test pieces before and after the friction test. In Figure 7(a), the existence of the CPB was not optically observed due to the high roughness of the substrate. Moreover, the topographical change of the worn surface on the block test pieces was not observed for all tribopairs. The results were supported by the results of the change of the surface roughness R_a ratio as shown in Figure 7(b) since there was no large difference between the roughness of the block test pieces before and after the friction test.

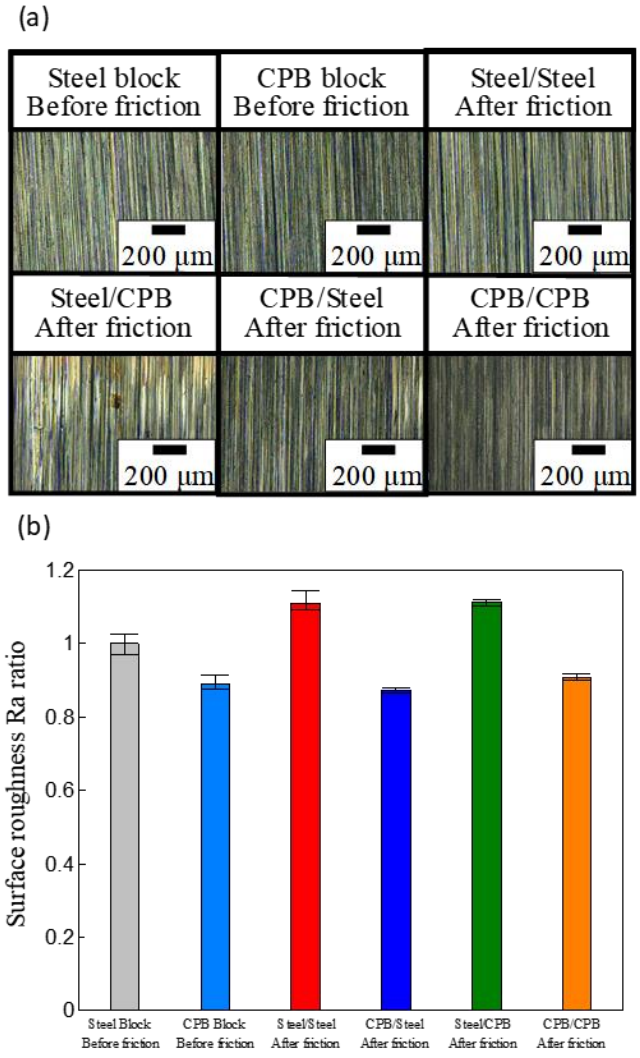

Figure 7: The topographical images (a) and the surface roughness R_a change of the block test pieces before and after the friction test (b).

3.2 Long-run friction test lubricated with the ionic liquid in mixed lubrication

To confirm the durability of the CPB lubricated with the ionic liquid in mixed lubrication, the long-run friction test was conducted under a load of 2 N at 0.8 m s^{-1} for the CPB/CPB and Steel/Steel tribopairs. Under this condition, the lubrication regime correspond to mixed lubrication regime from the results of Figure 3-6. Figure 8 shows the result of the long-run friction test for the CPB/CPB and Steel/Steel tribopairs. In Figure 8, the friction coefficient for the Steel/Steel gradually increased with the increment of the sliding distance and finally reached the value of 0.08. On the other hand, the CPB/CPB tribopair exhibited a lower friction coefficient than the Steel/Steel combination and a low friction coefficient of 0.005–0.008 for 1 h, which corresponds to the sliding distance of approximately 2.9 km. Figure 9 shows the SEM images and EDS element mapping images of the CPB grafted to the block test piece before and after the friction test. In Figure 9 (c) and (d), the red area which indicates the existence of carbon could correspond to the existence of the CPB layer on the block test piece in the EDS mapping images. Before the friction test, the red region was uniformly observed. This indicates that the CPB was coated uniformly on the block test piece. After the friction test, the red area partially disappeared, indicating that the CPB was partially worn out at the edge of the test piece. However, the red area in the middle of worn surface was clearly observed. Therefore, the CPB survived during the long-run friction test. From the results, the CPB has a high durability and extraordinary friction reduction effects in mixed lubrication.

4.0 DISCUSSIONS

The frictional characteristic of the CPB lubricated with the ionic liquid was investigated for the different conditions with various sliding speeds, sliding distance and tribopairs.

From the results of the Stribeck curves for all tribopairs, the configuration was one of the important factors for baring out the low friction potential of the CPB under our friction test condition. Figure 10 shows the result of the friction test on the 5th cycle for the tribopairs including the CPB modified test piece and on the 3rd cycle for the Steel/Steel tribopair. It should be noted that the super-low friction of the CPB was observed for the Steel/CPB and the CPB/CPB tribopairs at low sliding speed although the roughness of the steel substrate was relatively high. The super-low friction phenomenon could be coherentized as “hydrodynamic-like” behaviour of polymer brushes at low speed. The formation of EHL separating films at low sliding speeds could be supported by the stretched polymer chains in the ionic liquid, and the CPB-supported EHL separating film could be thicker than the substrate roughness, resulting in expanding a super-low frictional regime.

On the other hand, as shown in Figure 10, although the Steel/CPB gave low friction coefficient of 0.02 regardless of the sliding speed, the CPB/Steel tribopair did not show the low friction behaviour in the low speed regions. This difference can be explained by the difference of retention ability of the lubricant between the CPB and the steel. Figure 11 shows the difference between the wettability of the CPB and the steel for the ionic liquid. As shown in Figure 11, there were a large difference between the wettability of the CPB and the steel for the ionic liquid. For the steel, the contact angle was about 30 degrees, whereas the contact angle for the CPB was too small to measure. This indicates that the CPB has a much higher wettability compared to the steel for the ionic liquid. In other words, the CPB has high affinity for the ionic liquid. It is easily expected that the wettability of the sliding materials strongly related to the quantity of the lubricant on the sliding surface in our test configuration. This is because that it is possible a material excellent in

wettability carries a large amount of lubricant to sliding surface. Figure 12 shows the schematic illustration of the role of the CPB as a carrier of the ionic liquid under the configuration of our tribometer. As described above, the super-low frictional behaviour of the CPB at low sliding speeds was characterized as the formation of the CPB-supported EHL separating film. Based on this low frictional mechanism, the supply of the lubricant to the sliding surface is needed to form the low frictional separating film. For our configuration of the friction test, the ring test pieces provided the ionic liquid to the sliding contact area from a lubricant bath as the carrier. As shown in Figure 12 (a) and (b), the supply amount of the ionic liquid for the Steel/CPB tribopair could be much larger than the case of the CPB/Steel tribopair. This is because the CPB-coated ring test piece with high wettability could provide much larger amount of the ionic liquid to the sliding contact area from the lubricant bath than the case of the non-coated steel ring test piece. The amount of the ionic liquid at the contact area strongly influence not only the formation of the EHL separating film but also the swelling behaviour of the CPB. The well-swelled CPB are needed to form the EHL separating films at low speed since the film thickness of CPB in solvents depends on the degree of the swelling. In addition, friction characteristic of CPB is greatly affected by the degree of swelling (Nomura et al., 2011). This is the reason why the CPB/Steel (block/ring) tribopair did not show the low friction behaviour in the low speed regions while the Steel/CPB gave low friction behaviour regardless of the sliding speed. This is just a simple lubrication model of the CPB to explain the friction result in this configuration. It should be noted that friction phenomenon is affected by many factors (in this case, surface roughness, effects of the lubricant, free polymer generated by wear…). Thus, other approaches are needed to reveal the details of the low frictional mechanism of the CPB coated on the rough steel substrate.

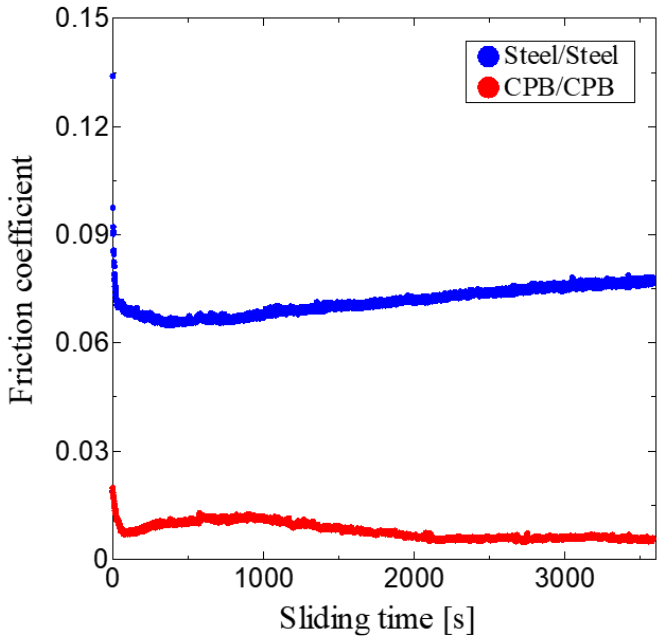

Figure 8: Time evolution of friction coefficient of Steel Steel and CPB/CPB tribopairs under a load of 2 N at the sliding speed of 0.8 ms^{-1}.

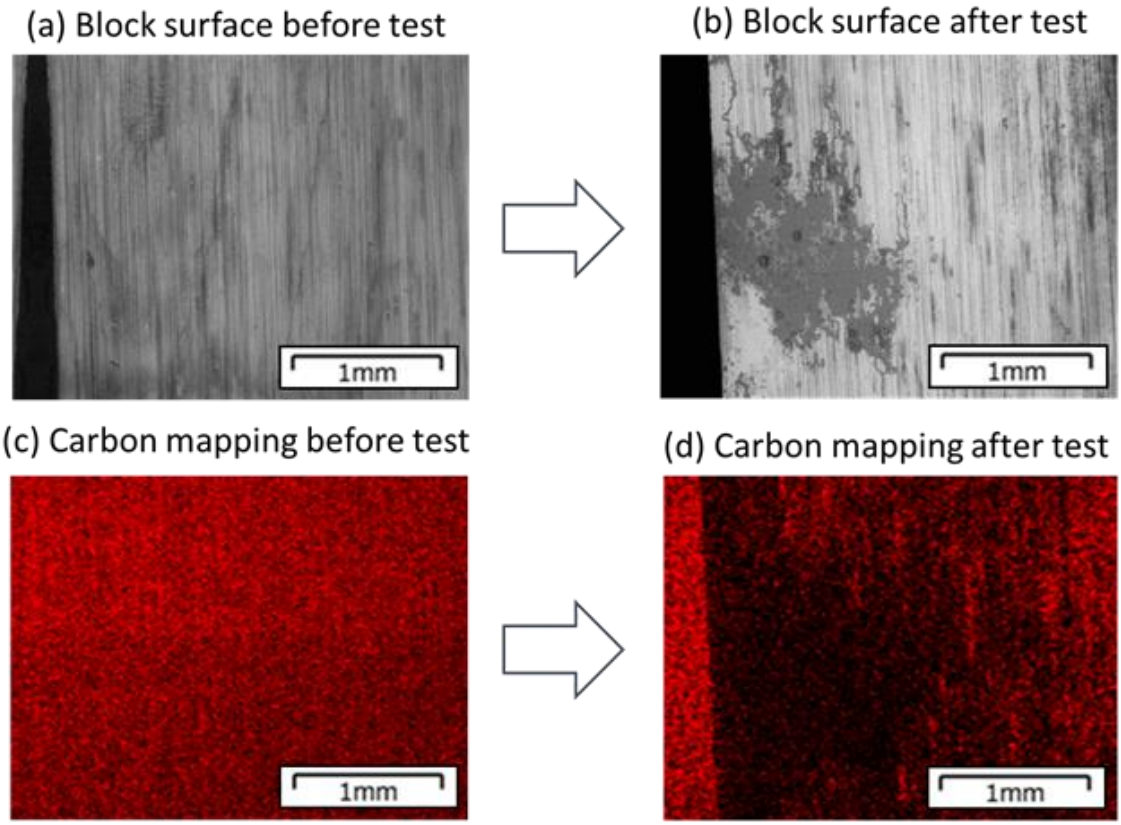

Figure 9: The surface observations of the CPB grafted to the block by mean of SEM-EDS. The images refer to (a) before friction test (b) after friction test (c) carbon mapping before friction test (d) carbon mapping after friction test.

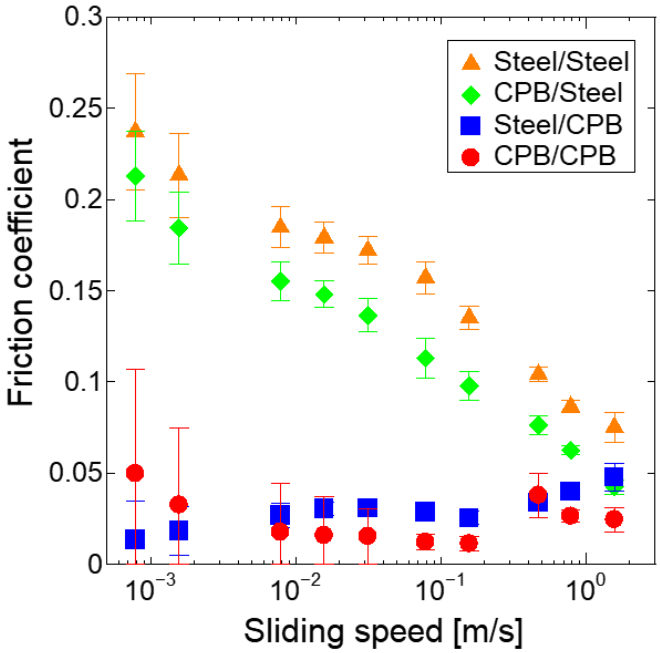

Figure 10: Sliding speed dependence of the friction coefficient of steel and the CPB in the ionic liquid under a load of 2 N at the sliding speed from 0.008ms^{-1} to 1.6 ms^{-1}. Combination of block and ring test pieces were ▲Steel/Steel, ◆CPB/Steel, ■Steel/CPB, and ●CPB/CPB, respectively.

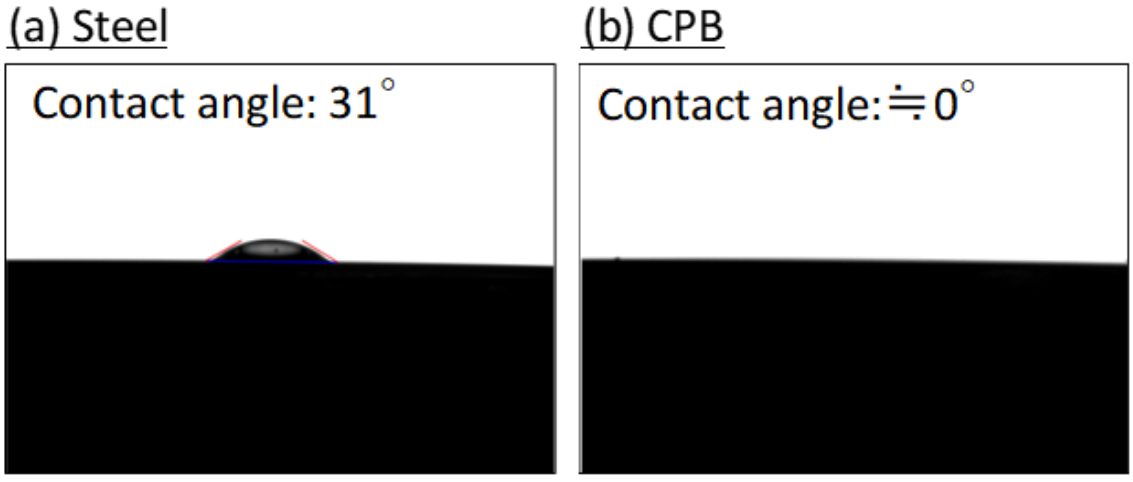

Figure 11: Evaluation of wettability of the ionic liquid to (a) steel (b) CPB.

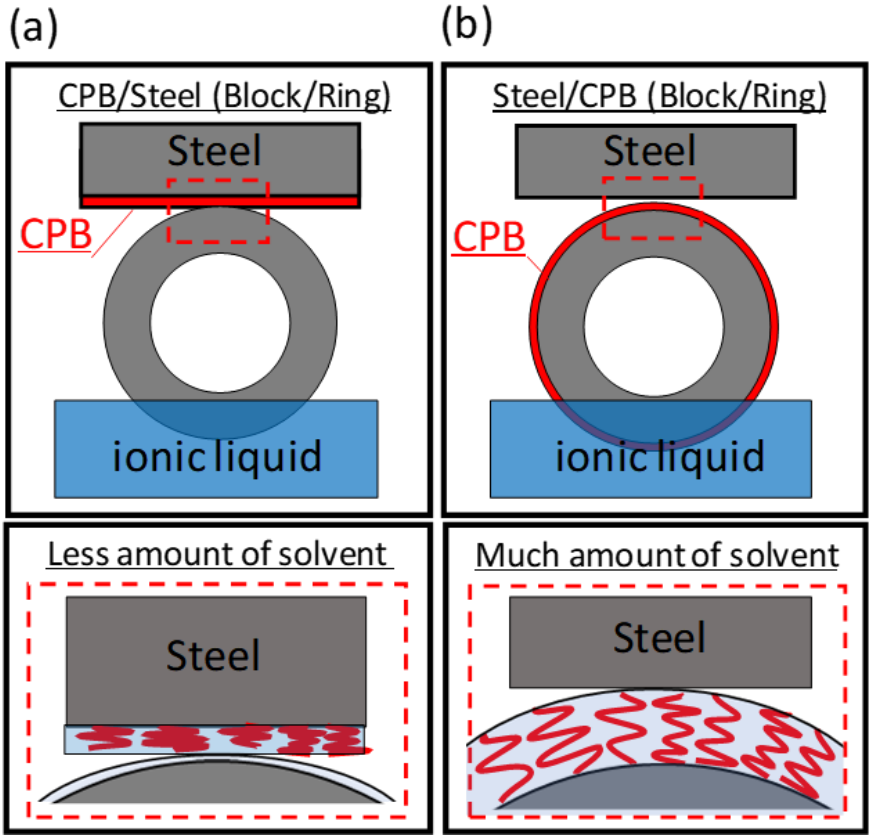

Figure 12: Schematic illustrations of the role of the CPB as a carrier of the ionic liquid.

5.0 CONCLUSION

We have investigated the macro-tribological properties of the CPB on rough steel under lubrication with the ionic liquid. The friction coefficient of the CPB-modified steel was lower than that of the unmodified steel. This was because that the CPB-supported EHL film was formed in the sliding contact area by modifying the CPB, which has high wettability for the ionic liquid, to the test pieces. In addition, the dependence of the friction coefficient on the sliding speed varied by the tribopairs. In the case of Steel/Steel and CPB/Steel, the friction coefficient decreased with the increment of the sliding speed. On the other hand, in the case of Steel/CPB and CPB/CPB, low friction coefficient was observed over a wide speed region. In the case of modifying the CPB to the ring test piece, much amount of the ionic liquid was supplied to the sliding contact area, and the CPB was easily swelled well. Therefore, the CPB-supported EHL separating film formed more, and the low friction coefficient was observed over a wide speed region in the case of modifying the CPB to the ring test piece. This result also implied that the macro-tribological properties of the CPB depend on the degree of swelling. From these results, we believe that thick CPB can exhibit good tribological performance in combination with an ionic liquid even on rough steel.

ACKNOWLEDGEMENT

This work was supported by the accel program from the Japan Science and Technology Agency, JST and JSPS KAKENHI Grand Numbers JP6630041.

REFERENCES

Allen, C. M. & Drauglis, E. (1969). BOUNDARY LAYER LUBRICATION: MONOLAYER OR MULTILAYER. Wear, 14, 363-384.

Hutching, I. M. (1992). Tribology: Friction and Wear of Engineering Materials. Butterworth-Heinemann.

Parnas, R. S., & Cohen, Y. (1994). A terminally anchored polymer chain in shear flow: Self-consistent velocity and segment density profiles. Rheologica Acta, 33, 485-505.

Klein, J. (1994). Shear of polymer brushes. Colloid and Surfaces A: Physicochemical and Engineering Aspects, 86, 63-76.

Klein, J., & Kumacheva, E. (1995). Confinement-induced phase transitions in simple liquids. Science, 2669(5225), 816-9.

Klein, J. (1996). Shear, friction, and lubrication forces between polymer-bearing surfaces. Annual Review of Materials Research, 26, 581-612.

Yang, W., & Zhou, F. (2017). Polymer brushes for antibiofouling and lubrication. Biosurface and Biotribology, 3, 97-114.

Chen, W., Cordero, R., Tran, H., & Ober, C. K. (2017). 50th Anniversary Perspective: Polymer Brushes: Novel Surfaces for Future Materials. Macromolecules, 50, 4089-4113.

Murdoch, T, J., Humphreys, B, A., Johnson, E, C., Webber, G, B., & Wanless, E, J. (2018). Specific ion effects on thermoresponsive polymer brushes: Comparison to other architectures. Journal of Colloid and Interface Science, 526, 429-450.

Klein, J., Kumacheva, E., Mahalu, D., Perehia, D., & Fetters, L. J. (1994). Reduction of frictional forces between solid surfaces bearing polymer brushes. Nature, 370, 634-636.

Klein, J., Kumacheva, E., Perehia, D., Mahalu, D., & Warburg, S. (1994). Interfacial sliding of polymer-bearing surfaces. Faraday Discussions, 98, 173.

Irfachsyad, D., Tildesley, D., & Malfreyt, P. (2002). Disspative particle dynamics simulation of grafted polymer brushed under shear. Physical Chemistry Chemical Physics, 4, 3008-3015.

Bielecki, R. M., Benetti, E. M., Kumar, D., & Spencer, N. D. (2012). Lubrication with Oil-Compatible Polymer Brushes. Tribology Letters, 45(3), 477-487.

Tsujii, Y., Nomura, A., Okayasu, K., Gao, K., Ohno, K., & Fukuda., T. (2009). AFM studies on microtribology of concentrated polymer brushes in solvents. Journal of Physics: Conference Series, 184, 1-7.

Sakata, H., Kobayashi, M., Otsuka, H., Takahara, A. (2005). Tribological Properties of Poly(methyl methacrylate) Brushes Prepared by Surface-Initiated Atom transfer Radical Polymerization. Polymer Journal, 37, 767-775.

Bielecki, R. M., Crobu, M., & Spencer, N. D., (2013). Polymer-Brush Lubrication in Oil: Sliding Beyond the Stribeck Curve. Tribology Letter, 49, 263-272.

Kobayashi, M., Kaido, M., Suzuki, A., & Takahara, A. (2016). Tribological properties of cross-linked oleophilic polymer brushes on diamond-like carbon films. Polymer, 7, 128-134.

Dupont, J., de Souza, R. F., & Suarez, P. A. Z. (2002). Ionic Liquid (Molten Salt) Phase Organometallic Catalysis. Chemical Reviews, 102, 3667-3692.

Freemantle, M. (2009). An introduction of Ionic Liquids. Royal Society of Chemistry.

Kirchner, B. (2010). Ionic Liquids. Springer Berlin Heidelberg.

Carmichael, A. J., Haddleton, D. M., Bon, S. A. F., & Seddon, K. R. (2000). Copper(Ⅰ) mediated living radical polymerization in an ionic liquid. Chemical Communications, 0, 1237-1238.

Biedron, T., & Kubisa, P. (2001). Atom-Transfer Radical Polymerization of Acrylates in an Ionic Liquid. Macromolecular Rapid Communications, 22, 1237-1242.

Susan, M. A., Kaneko, T., Noda, A., & Watanabe, M. (2005). Ion Gels Prepared by in Situ Radical Polymerization of Vinyl Monomers in an Ionic Liquid and Their Characterization as Polymer Electrolytes. Journal of the American chemical society, 127, 4976-4983.

Kubisa, P. (2009). Ionic liquids as solvents for polymerization processes — Progress and challenges. Progress in Polymer Science, 34, 1333-1347.

Liu, W., Ye, C., Gong, Q., Wang, H., & Wang, P. (2002). Tribological Performance of Room-Temperature Ionic Liquids as Lubricant. Tribology Letters, 13, 81-85.

Minami, I. (2009). Ionic Liquids in Tribology. Molecules, 14, 2286-2305.

Nomura, A., Ohno, K., Fukuda, T., Sato, T., & Yoshinobu, T. (2012). Lubrication mechanism of concentrated polymer brushes in solvents: effect of solvent viscosity. Polymer Chemistry, 3, 148-153.

Arafune, H., Kamijo, T., Honma, T., Sato, T., & Yoshinobu, T. (2015). A Robust Lubrication System Using an Ionic Liquid Polymer Brush. Advanced Materials Interfaces, 2, 1500187.

Werne, T., & Patten, T. E. (1999). Preparation of Structurally Well-Defined Polymer-Nanoparticle Hybrids with Controlled/Living Radical Polymerizations. Journal of the American chemical society, 121, 7409-7410.

Werne, T., & Patten, T. E., (2001), Atom Transfer Radical Polymerization from Nanoparticles: A Tool for the Preparation of Well-Defined Hybrid Nanostructures and for Understanding the Chemistry of Controlled/"Living" Radical Polymerization from Surfaces. Journal of the American chemical society, 123, 7497-7505.

Blomberg, S., Ostberg, S., Harth, E., Bosman, A. W., Horn, B., & Hawke, C. (2002). Production of crosslinked, hollow nanoparticles by surface- initiated living free-radical polymerization. Journal of Polymer Science Part A: Polymer Chemistry, 40, 1309-1320.

Pyun, J., Jia, S., Kowalewski, T., Patterson, G. D., & Matyjaszewski, K. (2003). Synthesis and Characterization of Organic/Inorganic Hybrid Nanoparticles: Kinetics of Surface-initiated Atom Transfer Radical Polymerization and Morphology of Hybrid Nanoparticle Ultrathin Films. Macromolecules, 36, 5094-5104.

Oliver, W. C., & Pharr, G. M. (1992). An improved technique for determining hardness and elastic modulus using load and displacement sensing indentation experiments. Journal of Materials Research, 7, 1564-1583.

Williams, D, L., Kuhn, A, T., Amann, M, A., Hausinger, M, B., Konarik, M, M., Nesselrode, E, L. (2010). Computerized Measurement of Contact Angles. Galvanotechnik, 101(11), 2502-2512.

Nomura, A., Okayasu, K., Ohno, K., Fukuda, T., & Tsujii, Y. (2011). Lubrication Mechanism of Concentrated Polymer Brushes in Solvents: Effect of Solvent Quality and Thereby Swelling State. Macromolecules, 44, 5013-5019.